Sensors and Materials, Vol. 30, No. 4 (2018) 821–832
MYU Tokyo

S & M 1541

Mechanical Vibration Fault Detection for Turbine Generator Using Frequency Spectral Data and Machine Learning Model: Feasibility Study of Big Data Analysis

Long-Yi Chang,[1,2*] Yi-Nung Chung,[2] Chia-Hung Lin,[2]
Jian-Liung Chen,[3] Chao-Lin Kuo,[4] and Shi-Jaw Chen[5]

[1]Department of Electrical Engineering, National Changhua University of Education, Changhua City, 50074, Taiwan
[2]Department of Electrical Engineering, National Chin-Yi University of Technology, Taiping District, Taichung City, 41170, Taiwan
[3]Department of Electrical Engineering, Kao-Yuan University, Lu-Chu District, Kaohsiung City, 82151, Taiwan
[4]Department of Maritime Information and Technology, National Kaohsiung Marine University, Cijin District, Kaohsiung City, 80543, Taiwan
[5]Department of Greenergy Science and Technology, Kao-Yuan University, Lu-Chu District, Kaohsiung City, 82151, Taiwan

(Received October 23, 2017; accepted December 26, 2017)

Keywords: vibration signal, mechanical vibration fault, frequency spectral data, radial-based color relation analysis

The frequency spectra of vibration signals can be used to monitor the mechanical conditions of a turbine generator. Frequency-based features are extracted by fast Fourier transformation (FFT). The changes in frequency spectral data and amplitude are used to separate the normal condition from the fault conditions. These features indicate that the characteristic frequencies are $1 \times f$, $2 \times f$, $3 \times f$, and two other frequency bands, $< 0.4 \times f$ and $> 3 \times f$, where the frequency f is the rotor frequency. The power spectral data shows the mechanical vibration fault at particular characteristic frequencies. Then, radial-based color relation analysis (CRA) is applied to identify mechanical faults, including normal condition, oil-membrane oscillation, imbalance, and no orderliness. Using practical records, the experimental results will show that the proposed method has a higher accuracy in mechanical vibration fault detection.

1. Introduction

A turbine generator is a major component of thermal plants, hydroelectric plants, or wind farms, consisting of several parts: turbine, generator, shaft (low speed or high speed), and exciter. A steam turbine can also be divided into high-pressure (HP), low-pressure (LP), and intermediate-pressure (IP) parts, which are girdled by bearings and provide most of the diagnostic information, as seen in Fig. 1(a). A wind turbine generator converts electrical power using rotor blades and wind speed, including vertical and horizontal axis types, as seen in Fig.

*Corresponding author: e-mail: lychang@mail.ncut.edu.tw
http://dx.doi.org/10.18494/SAM.2018.1783

ISSN 0914-4935

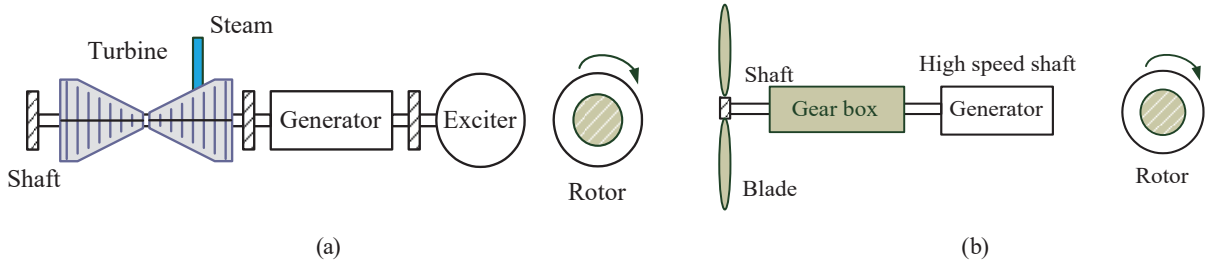

Fig. 1. (Color online) The diagram of turbine generators. (a) Steam turbine generator and (b) wind turbine generator.

1(b). Owing to data transmission problems (outdoor environment), accelerometers, and strain gages are used to monitor the gear box for mechanical condition detection. Digital image and stereo-photogrammetry are also used to measure the dynamic conditions.[1,2] For a steam turbine with a large-scaled capacity, the mechanical dysfunctions may damage the generator and cause outages and community profit loss. Therefore, it is necessary to detect faults early and take immediate action to avoid profit loss.

The turbine generator faults can be classified into three types, namely electrical fault, mechanical vibration fault, and cooling system fault. The first two are the common incipient faults in the turbine generator. Electrical faults are rotor excitation short circuit, stator winding ground fault, and stator winding short circuit involving the three-phase fault or line-to-line fault.[3] Rotor excitation short circuit may cause an unbalanced magnetic pull that acts on the rotor and stator to cause vibrations. When a short circuit occurs on the stator winding, a percentage-differential relay quickly trips the main circuit breaker. Mechanical faults could be caused by stresses involved in the conversion of mechanical energy to electrical energy. Machine bearings may be damaged by inadequate lubrication, impure lubrication, or incorrect loading.[4] On-line monitoring devices, such as the shaft position meter, shaft vibration meter, accelerometer, and displacement meter, can be used to detect the operation conditions. Two proximity sensors are mounted parallel to the axis of rotation to monitor the axial displacements. Two accelerometers per bearing are mounted on two perpendicular axes, and measure absolute vibration signals involving the frequency ranges of 10–10000 Hz. Hence, the power frequency spectra of the vibration signals are important information to detect the faults.[5,6] Frequency techniques, such as wavelet analysis and fast Fourier transform (FFT),[7] are used to extract the frequency features, which are changes in frequency and amplitude and are dependent on the fault types between 10 and 1000 Hz. Then, artificial intelligent techniques (machine learning models) can provide promising results to identify the vibration features in a turbine generator, such as artificial neural networks, fuzzy neural networks, and wavelet neural networks.[8–11]

From practical records, big data analysis and collection can extract the key frequency features to separate the normal condition from any fault. The characteristic features are extracted using the FFT method, including the frequencies $1 \times f$, $2 \times f$, $3 \times f$, ..., and $9 \times f$, where the frequency f is 60 Hz. To develop an assistant tool, the frequency spectral data analysis and radial-based color relation analysis (CRA)[12–15] are carried out with a machine learning model

to monitor the mechanical vibration faults. Among multidimensional big data, the radial-based function is a kernel model with Gaussian functions to measure dissimilarity and similarity degrees, which are parameterized into the specific membership grades for pattern recognition. Then, a CRA-based decision making algorithm is applied to detect turbine generator faults. It is employed to map membership grades into hue angle and saturation value in hue–saturation–value (HSV) color space, with descriptive perceptual color relationships for identifying normal condition, oil-membrane oscillation, imbalance, and no orderliness. Experimental results will show that the proposed method demonstrates a good computational efficiency, easy implementation, and a high accuracy for practical uses.

2. Materials and Methods

2.1 Frequency feature extraction

A vibration signal or waveform is an important indicator for monitoring defects. Vibration signals are collected from a data acquisition system. The time-domain signals from accelerometers are extracted and converted into frequency-domain features by the FFT method. FFT is an approach with a two-sided spectrum in a complex form (real and imaginary parts), which can be scaled and converted to the polar form to obtain the amplitude and phase, as

$$f(e^{j\Omega}) = \sum_{n=-\infty}^{\infty} x[n]e^{-j\Omega n}, \tag{1}$$

where $x[n]$ is a discrete-time domain vibration signal (sample data); n is the sampling points; $y(e^{j\Omega})$ is the periodic and extends from the frequency 0 to the sampling frequency f_s. The amplitude of the FFT is

$$f = [f_1, f_2, ..., f_n, ..., f_N] = \frac{abs(f)}{\max[abs(f)]}, \tag{2}$$

where the element f_n, $n = 1, 2, 3, \ldots, N$, is the amplitude of the frequency spectrum. With the frequency-domain features, diagnostic analysis is used to detect faults in characteristic frequencies associated with various fault types. For 80 practical records, the frequency spectrum can be estimated (characteristic frequencies, $80 \times 9 = 720$), including characteristic frequencies and amplitudes. The frequency features are $n \times f$, rotor frequency $f = 60$ Hz, order $n = 1, 2, 3, \ldots, 9$ ($N = 9$ in this study), as seen in Fig. 2. According to the frequency patterns, training data can be generated to construct the machine learning model with the frequency spectral data of vibration signals. Different fault types appear with their symptomatic patterns and are divided into

· Class 1: "Oil-membrane oscillation" with the total number of 20;
· Class 2: "Imbalance" with the total number of 20;
· Class 3: "No orderliness" with the total number of 20;

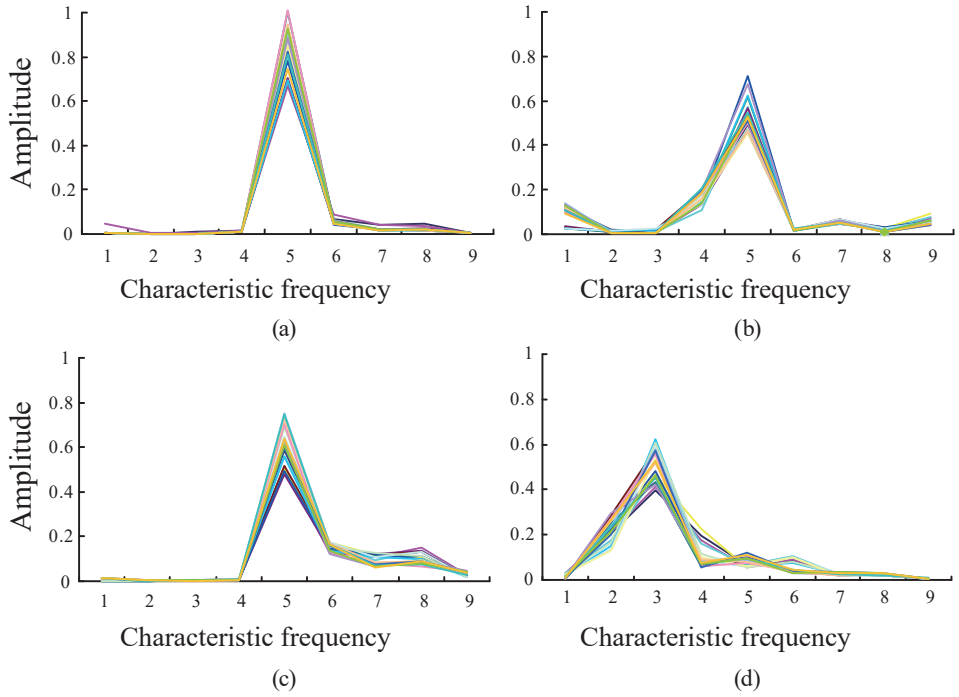

Fig. 2. (Color online) Frequency features. (a) Oil-membrane oscillation, (b) imbalance, (c) no orderliness, and (d) normal condition.

· Class 4: "Normal" with the total number of 20.

As a digital signal processing algorithm, diagnostic algorithms can be easily realized in a PC-based device or an embedded system. In this paper, the radial-based CRA algorithm is developed with frequency spectral data for the feasibility study of big data analysis.

2.2 Radial-based CRA

For high-dimensional recognition applications, the radial-based function network establishes a nonlinearity estimator with more input variables, which can model a high-dimensional pattern mechanism with various available combinations of training patterns, as seen in Fig. 3. Based on similarity and dissimilarity, relational measurement is a manner for pattern recognition between the reference pattern f_r and the other comparative patterns f_c. For pattern recognition between the reference pattern, $f_r(0) = [f_1(0), f_2(0), \ldots, f_n(0), \ldots, f_N(0)]$, and other comparative patterns, $f_c(k) = [f_1(k), f_2(k), \ldots, f_n(k), \ldots, f_N(k)]$. The radial-based function (Gaussian function) G is used to measure similarity degree and is parameterized as[12]

$$G(k) = \exp\left[\frac{-1}{2\sigma^2} \times \left(\sqrt{\sum_{i=1}^{N} (\Delta f_i(k))^2}\right)^2\right], \tag{3}$$

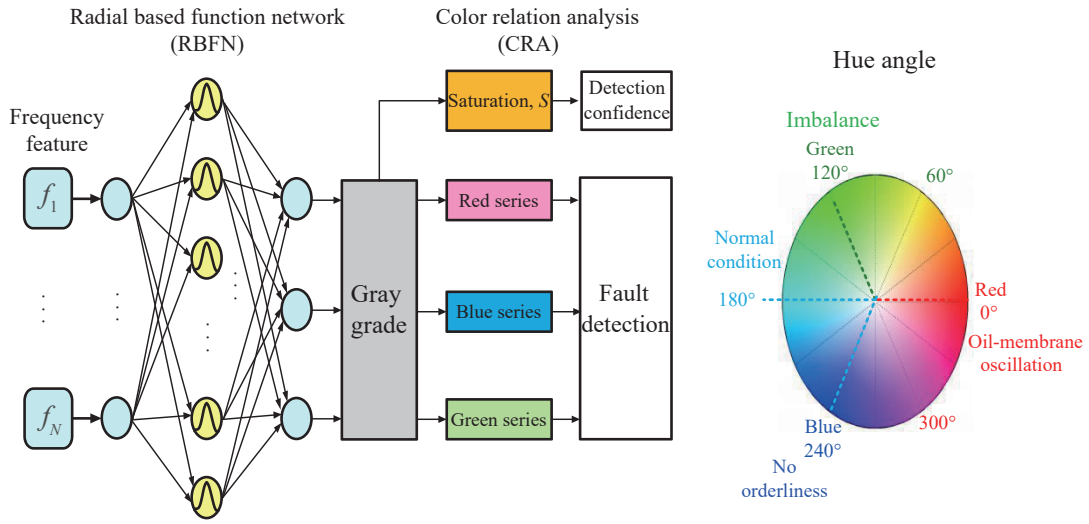

Fig. 3. (Color online) Radial based color relation analysis and HSV color space for mechanical faults.

$$ED(k) = \sqrt{\sum_{i=1}^{N} (\Delta f_i(k))^2}, \quad \Delta f_i(k) = |f_{ri}(0) - f_{ci}(k)|, \tag{4}$$

where K is the number of training data, $k = 1, 2, 3, \ldots, K$; $ED(k)$ is the Euclidean distance (ED); σ is the standard deviation and $\sigma = 0.1$ is chosen in this study. The Gaussian functions G are used to classify these patterns. The similarity degree is parameterized with Eqs. (3) and (4), and is employed to screen the similarity degree among the training patterns, varying within between value 0 and 1. If input feature pattern is similar to any comparative pattern, the $ED(k)$ will be small values, as $ED(k) \to 0$ and $G(k) \to 1$, otherwise, $ED(k) \gg 0$ and $G(k) \to 0$. Then, the average similarity degree for each desired class is

$$y_j(k) = \sum_{k=1}^{K} w_{kj} \times G(k) \Big/ \sum_{k=1}^{K} G(k), \tag{5}$$

where the values of $w_{kj} \in [0, 1]$ are weighted connections for the four classes, $j = 1, 2, 3, 4$. Then, the minimum and maximum average grades are

$$\rho_{min} = \min[y_1, y_2, y_3, y_4], \tag{6}$$

$$\rho_{max} = \max[y_1, y_2, y_3, y_4], \tag{7}$$

$$\Delta\rho = \rho_{max} - \rho_{min}, \tag{8}$$

where $\rho_{m,min} \neq \rho_{m,max}$ and $\rho_{max} \neq 0$.

According to the HSV color model,[13–15] the CRA model is defined as a transformation manner from the similarity degrees to the HSV color space. As seen in Fig. 3, the hue angle $h \in [0, 360°]$ can be defined as

$$h = \begin{cases} 0 \text{ or } 360, \ \rho_{\max} = y_1 \\ 180, \ \rho_{\max} = y_4 \\ 180 - 60 \times (\frac{y_2 - y_4}{\Delta\rho}), \ \rho_{\max} = y_2 \\ 180 + 60 \times (\frac{y_3 - y_4}{\Delta\rho}) + 240, \ \rho_{\max} = y_3 \end{cases} \tag{9}$$

where $\rho_{min} = \rho_{max}$ and $h = 0$. The saturation s and the value v are found, which are defined as

$$s = 1 - \frac{\rho_{min}}{v}, \ v = \rho_{max}, \ \rho_{max} \neq 0. \tag{10}$$

The index h is used to identify the four classes, as four open intervals as follows: (1) $h = 0°$ or 360° is red series color for oil-membrane oscillation; (2) $h_m = 180°$ is light blue series color for normal condition; (3) $h = 120°$ is green series color for imbalance; and (4) $h = 240°$ is blue series color for no orderliness. The index s is also employed to provide the confidence level. If its value is > 0.5 and approaches 1.0, we have a high confidence to confirm the possible class. The CRA is a visual method with color codes to represent the fault types and has a flexibility inference mechanism.

The proposed fault detection procedure consists of four stages: (a) vibration signal measurement, (b) feature extraction by FFT method, (c) feature pattern combination, and (d) fault detection using radial based CRA, as seen in Fig. 4. Vibration signals from the accelerometer metering system are collected and transferred to the computer. Frequency-domain features are extracted by the FFT method. The fault patterns can be revealed using frequency spectral data in big data analysis, as seen at 120, 180, 300, 360, and 420 Hz in Fig. 5. Abnormal condition can be detected at the pattern recognition stage using radial-based CRA.

3. Results

The proposed diagnostic procedure was designed and tested using LabVIEW (National Instruments™ Corporation, Austin, Texas, USA) graphical programming software and MATLAB software/math-script workspace (MathWorks, Natick, Massachusetts, USA). An embedded system (National Instruments™ myRIO-1900, Austin, Texas, USA) was also used to implement the prototype model including: (1) metering the electrical signals (vibration signals), (2) extracting the frequency feature using FFT algorithm, and (3) designing the radial-based CRA in a programmable processor; as seen in Fig. 6. The measurement data was divided into two groups; 80 frequency-based patterns were used as the training data and the other 80 patterns were used as testing data.

Using practical records, the proposed procedure provided highly confident results for decision making in fault detection. The MATLAB colormap function represented the experimental results to the HSV color space between 0° and 360°. For the 80 testing data, the

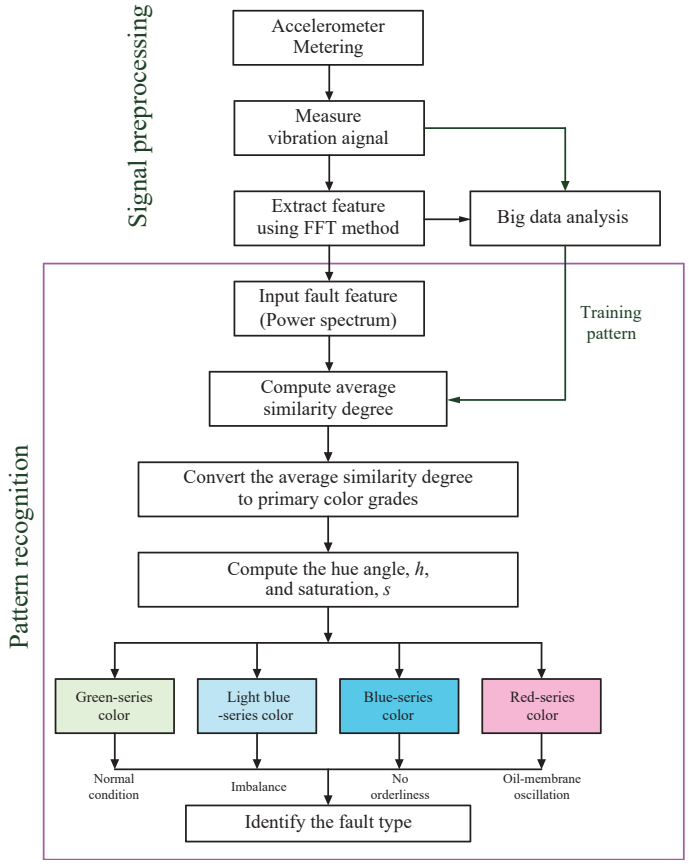

Fig. 4. (Color online) The flowchart of mechanical vibration fault detection.

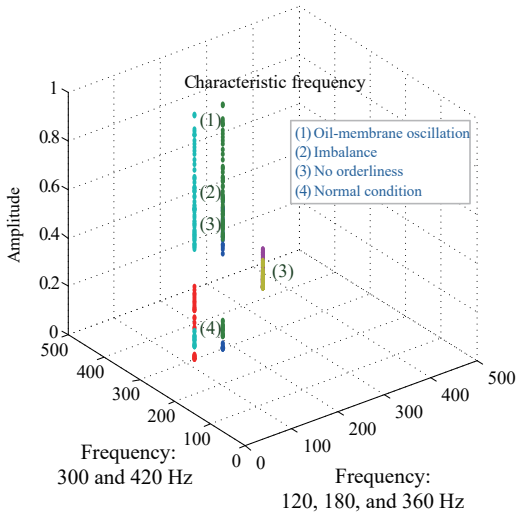

Fig. 5. (Color online) Frequency domain features in key characteristic frequencies (120, 180, 300, 360, and 420 Hz).

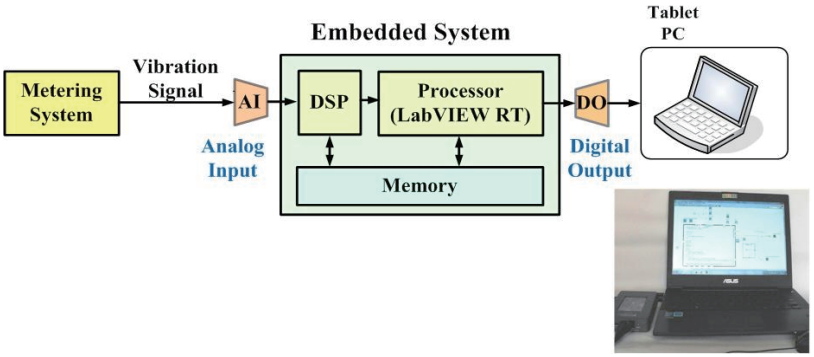

Fig. 6. (Color online) Prototype design in an embedded system.

experimental results indicated that the hue angles appeared at 0° or 360°, 180°, 120°, and 240° to identify the fault types, as shown in Fig. 7. There were 20 records of oil-membrane oscillation (No.1#–No.20#), 20 records of imbalance (No.21#–No.40#), 20 records of no orderliness (No.41#–No.60#), and 20 records of normal condition (No.61#–No.80#). For example, an oil-membrane

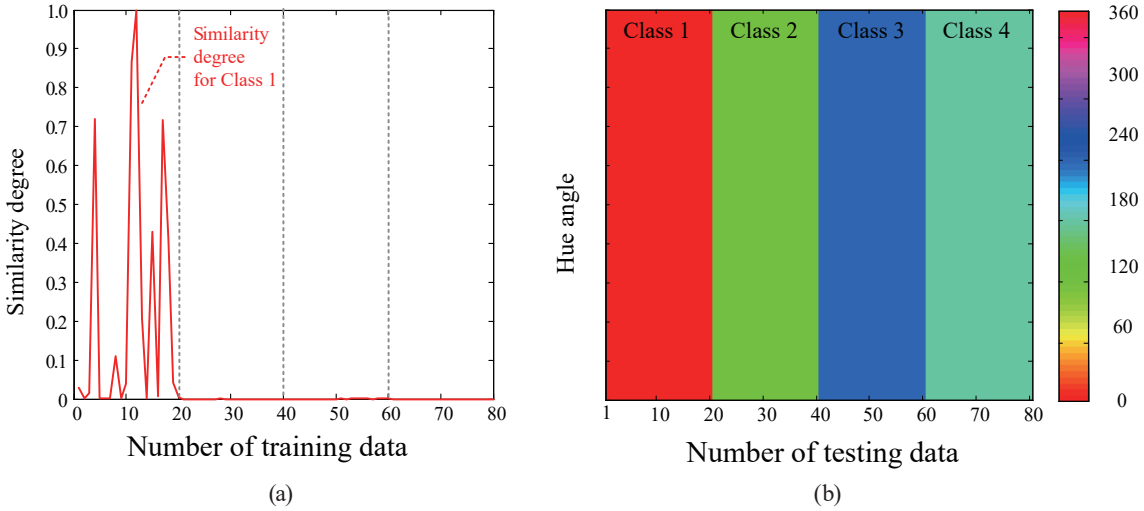

Fig. 7. (Color online) Experimental results from 80 testing data. (a) Similarity degree measurements and (b) experimental results obtained using color perceptual representations.

oscillation event (No. 11#) was investigated. The diagnostic procedures are as follows:

Step (1) given the frequency spectral pattern of vibration signal, f = [0.0058, 0.0016, 0.0011, 0.0110, 0.8479, 30.0501, 0.0218, 0.0222, 0.0030];

Step (2) compute the similarity degrees using Eqs. (3) and (4) as shown in Fig. 7(a);

Step (3) compute the average similarity degrees using Eq. (5), y = [1.0000, 0.0000, 0.0000, 0.0000];

Step (4) convert the average similarity degrees to the hue angle and saturation, h = 0°/360° and s = 1.0000, respectively. The overall experimental results obtained using color perceptual representations are shown in Fig. 7(b).

The MATLAB images and colormap functions scaled the experimental results to the HSV color space and displayed the visual image. For record No. 11#, the hue angle h = 0°/360° and saturation s = 1.0000 indicated the possible fault, and confirmed that the fault is an "oil-membrane oscillation" event. The radial-based CRA model promised the results with 100% accuracy. To demonstrate the effectiveness of the proposed method, twenty recorded data from steam-turbine generator sets are tested as shown in Table 1.[7] There are 6 records of oil-membrane oscillation (Nos. 1–6), 6 records of imbalance (Nos. 7–12), 6 records of no orderliness (Nos. 13–18), and 6 records of normal condition (Nos. 19–24). The input data include the five amplitude values of the vibration spectrum. Table 1 shows the frequency spectrum for the test records. The radial-based CRA method promises the results with 100% accuracy.

To test the robustness of the proposed method, testing data were produced with −50 to +50% noises. Figure 8 shows the detection accuracies versus adding noises for the same testing data involving oil-membrane oscillation, imbalance, no orderliness, and normal condition. The proposed method did not promise the results with 100% accuracy owing to added serious noises. The results showed that the proposed method had high detection accuracies under noisy background with −15 to +20% noises (Accuracy > 80%). In addition, artificial neural networks

Table 1
Testing data of steam-turbine generator sets.

Generator number	f_1	f_2	f_3	f_4	f_5	f_6	f_7	f_8	f_9	h (Hue)	s
1	0.0027	0.0014	0.0082	0.0155	0.9235	0.0687	0.0404	0.0459	0.0045	0	1
2	0.0458	0.0028	0.0027	0.0172	0.6685	0.0888	0.0402	0.0367	0.0063	0	1
3	0.0043	0.00157	0.0015	0.0110	0.6920	0.0510	0.0181	0.0169	0.0029	0	1
4	0.0040	0.0016	0.0014	0.0118	0.9279	0.0458	0.0200	0.0198	0.0038	0	1
5	0.0057	0.0014	0.0014	0.0090	0.8228	0.0550	0.0207	0.0199	0.0028	0	1
6	0.0053	0.0015	0.0014	0.0101	0.8061	0.0511	0.0169	0.0226	0.0026	0	1
7	0.1193	0.0187	0.0079	0.1322	0.4925	0.0192	0.0440	0.0262	0.0737	120	1
8	0.1310	0.0137	0.0071	0.1322	0.4743	0.0202	0.0463	0.0204	0.0716	120	1
9	0.0301	0.0124	0.0204	0.1970	0.5295	0.0189	0.0671	0.0208	0.0482	120	1
10	0.0256	0.0108	0.0188	0.1416	0.6207	0.0219	0.0547	0.0286	0.0583	120	1
11	0.1197	0.0064	0.0049	0.1577	0.4647	0.0197	0.0491	0.0124	0.0435	120	1
12	0.1068	0.0048	0.0054	0.1998	0.5084	0.0218	0.0541	0.0109	0.0428	120	1
13	0.0015	0.0017	0.0032	0.0064	0.5587	0.1747	0.0923	0.1351	0.0255	240	1
14	0.0021	0.0016	0.0032	0.0053	0.4778	0.1432	0.1223	0.1349	0.0182	240	1
15	0.0016	0.0018	0.0029	0.0058	0.6919	0.1542	0.1280	0.1112	0.0200	240	1
16	0.0139	0.0025	0.0027	0.0059	0.6169	0.1612	0.0771	0.0917	0.0329	240	1
17	0.0140	0.0021	0.0034	0.0062	0.5955	0.1598	0.0749	0.0871	0.0382	240	1
18	0.0119	0.0023	0.0029	0.0076	0.7486	0.1638	0.0682	0.0766	0.0303	240	1
19	0.0158	0.2163	0.4644	0.0699	0.0971	0.0323	0.0332	0.0282	0.0068	180	1
20	0.0113	0.2680	0.5287	0.0763	0.1119	0.0428	0.0307	0.0323	0.0067	180	1
21	0.0055	0.2851	0.4319	0.0650	0.0995	0.0378	0.0266	0.0255	0.0047	180	1
22	0.0043	0.2859	0.5788	0.0581	0.0850	0.0341	0.0281	0.0252	0.0060	180	1
23	0.0054	0.2488	0.4302	0.0609	0.0911	0.0423	0.0238	0.0221	0.0049	180	1
24	0.0045	0.2241	0.4807	0.0852	0.0930	0.0392	0.0265	0.0269	0.0065	180	1

Note: f is the frequency of the generator rotor.

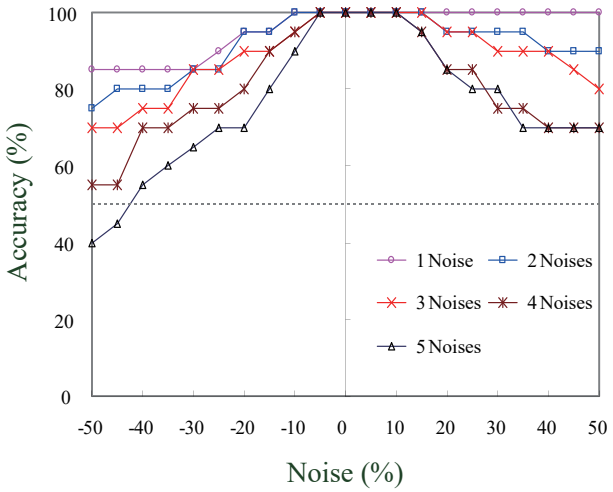

Fig. 8. (Color online) Detection accuracy versus adding −50 to +50% noises.

had some limitations in dealing with high-dimensional training data including learning processes, iteration computations for determining weights and learning rates, and network architecture determinations, which is difficult to retrain with new training data. In contrast to

artificial neural networks, the proposed method had a straightforward mathematical operation to process numerical data without any inference rules, and requires no iterative and recursive computations for adjusting many parameters. With the same experimental data, the proposed method showed better performance than traditional methods, and confirmed the higher confidence of detection results in the tests with and without noises.

4. Conclusions

The integrating FFT and radial-based CRA has been presented for mechanical vibration fault detection in turbine generators. The proposed method could effectively detect mechanical condition with the frequency spectra of vibration signals. The frequency features were extracted by the FFT method. In the feasibility study of big spectral data analysis, these key frequency features were at 120, 180, 300, 360, and 420 Hz. Characteristic frequencies with orders 1 to 9 (60–540Hz) were combined with various feature patterns to separate the normal condition from any fault type. The proposed radial-based CRA method could avoid the determination of the network architectures, parameter assignments, and iteration computations. Mathematical operation required less computation time for processing numerical data without adjusting any parameters. For both testing data without noise or with −15 to +20% noisy backgrounds, the experimental results demonstrated the efficiency of the proposed method. Compared with other artificial neural networks, the proposed method showed good performance for fault diagnosis in turbine generators. To develop an assistance tool, the proposed method is easy to implement in a portable device and a hardware device, can be further constructed in an on-line model, and be integrated into the monitoring instrument.

Acknowledgments

This work was supported in part by the Ministry of Science and Technology, Taiwan, under contract number: MOST 105-2634-F-244-001, duration: November 1, 2016–October 31, 2017. We thank Dr. Chien-Hsien Wu for sharing his experiences in vibration diagnosis for turbine generators.

References

1 J. Baqersad, C. Niezrecki, and P. Avitabile: Mech. Syst. Sig. Process. **62**–**63** (2015) 284.
2 Lundstrom, J. Baqersad, C. Niezrecki, and P. Avitabile: Conf. Proc. Society Experimental Mechanics Series (2012) 269.
3 S. Wan, H. Li, and Y. Li: Artif. Intell. Eng. **4** (1996) 335.
4 X. Wang and S. Yang: Artif. Intell. Eng. **4** (1996) 342.
5 M. Kawada, K. Yamada, K. Yamashita, and K. Isaka: Power Syst. Conf. Exposition **13** (2004) 1215.
6 H. Elmaati, A. Benbouaza, B. Elkihel, and F. Delaunois: Int. J. Emerging Trends Technol. Comput. Sci. **2** (2013) 240.
7 M.-H. Wang: IEE Proc.-Gener. Transm. Distrib. **151** (2004) 503.
8 K. Shanlin, Z. Huanzhen, and K. Yuzhe: 2009 Int. Conf. Mechatronics Automation (2009) 4414–4418.
9 C.-P. Huang, W.-G. Liu, and H.-Z. Su: Emerging Intell. Comput. Technol. Appl. **5754** (2009) 724.
10 M. Rahmoune, A. Hafaifa, and M. Guemana: 2015 3rd Int. Conf. Control, Engineering & Information Technology (2015).

11 G. S. Galloway, V. M. Gatterson, T. Fay, A. Robb, and G. Love: Proc. 3rd European Conf. Prognostics and Health Management Society (2016) 172.
12 D. F. Specht: IEEE Trans. Neural Network **2** (1991) 568.
13 C.-H. Lin: Comput. Methods Programs Biomed. **103** (2011) 121.
14 W.-L. Chen, C.-D. Kan, and C.-H. Lin: IET Cyber-Physical Systems: Theory Appl. **2** (2017) 10.
15 C.-H. Lin, M.-S. Kang, C.-H. Huang, and C.-L. Kuo: Int. Conf. Computer, Electrical, System Science, and Engineering (2010) 818–824.

About the Authors

Long-Yi Chang received his B.S. degree in Electrical Engineering from Chin-Yi Institute of Technology and Commerce, Taichung, Taiwan, in 1992, and his M.S. degree in Automatic Control Engineering from Feng Chia University, Taichung, Taiwan, in 2003. He has been working toward his Ph.D. in Electrical Engineering at National Changhua University of Education, Changhua, Taiwan, since 2014. He is presently an assistant professor at National Chin-Yi University of Technology, Taichung, Taiwan. His areas of interest include distribution system design, renewable energy, electrical energy management, and energy-conservation technology.

Yi-Nung Chung received his B.S. degree in electrical engineering from National Cheng Kung University, Tainan, Taiwan, in 1981, his M.S. degree in electrical engineering from Lamar University, Beaumont, TX, in 1986, and his Ph.D. degree from the Department of Electrical Engineering, Texas Tech University, Lubbock, TX, in 1990. He is currently a professor in the Department of Electrical Engineering, National Changhua University of Education, Changhua, Taiwan. His research interests include renewable energy, solar energy system, signal processing, and image processing.

Chia-Hung Lin was born in 1974. He received his B.S. degree in Electrical Engineering from Tatung Institute of Technology, Taipei City, Taiwan, in 1998, his M.S. degree in Electrical Engineering from the National Sun Yat-Sen University, Kaohsiung City, Taiwan, in 2000, and the Ph.D. degree in Electrical Engineering from National Sun Yat-Sen University in 2004. Currently, he is a professor in the Department of Electrical Engineering, National Chin-Yi University of Technology, Taichung City, Taiwan, where he has been since 2018. His research interests include fault diagnosis in power systems, neural network computing and its applications, harmonic analysis, biomedical signal processing, and pattern recognition.

Jian-Liung Chen received his Ph.D. degree in Electrical Engineering from National Sun Yat-Sen University in 2003. Currently, he is an associate professor in the Department of Electrical Engineering, Kao-Yuan University, Kaohsiung City, Taiwan, where he has been since 2010. His research interests include LMI approach in control, robust control, descriptor system theory, digital signal processing, intelligent control systems, and pattern recognition.

Chao-Lin Kuo received his B.S. degree from the department of Automatic Control Engineering, Feng Chia University, Taichung City, Taiwan, in 1998, and his M.S. degree from the Institute of Biomedical Engineering, National Cheng Kung University, Tainan City, Taiwan, in 2000. In 2006, he received his Ph.D. degree from the Department of Electrical Engineering, National Cheng Kung University, Tainan City, Taiwan, in 2006. Currently, he is an associate professor of Department of Maritime Information and Technology, National Kaohsiung Marine University, Kaohsiung City, Taiwan, where he has been since 2011. His current research interests include intelligent control systems, fuzzy systems, embedded systems, and their applications.

Shi-Jaw Chen received his M.S. and Ph.D degrees in Electrical Engineering from the National Sun Yat-sen University, Kaohsiung City, Taiwan, in 1993 and 2001, respectively. Currently, he is an associate professor in the Department of Greenergy Science and Technology, Kao Yuan University, Kaohsiung City. His research interests include distribution system state estimation, renewable energy, energy management, power system operations, and artificial intelligent applications in power systems.